Vol.4, No.2, Page 1682- 1693, 2026 https://doi.org/10.59628/jast.v4i2.2576 ISSN 2958-9568 JAST

SUN PUBLISHER

مجلة جامعة صنعاء للعلوم التطبيقية والتكنولوجيا

Sana'a University Journal of Applied Sciences and Technology

https://journals.su.edu.ye/index.php/jast/

Efficient Numerical Method for Solving a Cancer Tumor Model Governed by Fractional Partial Differential Equations Involving the ψ-Caputo derivative

S.M. Al-Mekhlafi *

Department of Mathematics, Faculty of Education, Sana'a University, Sana'a, Yemen.

*Corresponding author: sih.almikhlafi@su.edu.ye

Abstract

This paper introduces a novel fractional-order framework for modeling tumor-immune-drug interactions using Ψ-Caputo derivatives with general memory kernels. Unlike classical approaches, our model captures hereditary effects and anomalous transport inherent in cancer biology through flexible time-scaling laws. We establish rigorous theoretical guarantees, including existence, uniqueness, non-negativity, and boundedness of solutions, ensuring biological feasibility. Numerically, we develop a fully implicit θ-method with Ψ-Caputo discretization, proving unconditional stability and demonstrating its efficacy through comprehensive simulations. Our results reveal how the fractional order ξ and kernel selection critically regulate tumor persistence, immune activation, and treatment outcomes, uncovering memory-driven dynamics inaccessible to integer-order models. This work demonstrates that Ψ-Caputo operators are a powerful tool for predictive oncology, bridging fractional partial differential equation theory with cancer systems biology.

Article Info

Keywords:
Fractional partial differential equations, Ψ-Caputo derivative, Cancer modeling, Stability analysis, Numerical methods, Tumor–immune–drug dynamics

Article History:
Received: 27-November-2025,
Revised: 29-November-2025,
Accepted: 30-December-2025,
Published: 28 February 2026.

1. INTRODUCTION

Cancer remains one of the leading causes of morbidity and mortality worldwide, with tumor progression and therapeutic response governed by highly nonlinear, multiscale, and memory-driven biological processes [1–3]. The complex interplay between tumor cells, immune response, and chemotherapeutic agents has motivated the development of mathematical models to gain predictive insights and optimize treatment strategies. Classical models based on systems of ordinary or partial differential equations (ODEs/PDEs) have offered important advances [4, 5], yet their reliance on integer-order derivatives often limits their ability to capture hereditary and anomalous dynamics inherent in cancer biology.

Fractional calculus has recently emerged as a powerful mathematical tool for describing nonlocality, long-range dependence, and memory effects in complex systems [6, 7]. In oncology, fractional-order models have been successfully applied to tumor–immune interactions [8, 9], angiogenesis [10], and drug delivery dynamics [11]. By introducing memory kernels into the governing equations, fractional models provide more realistic representations of cell–cell interactions, immune delays, and treatment effects that cannot be captured by classical integer-order approaches.

Among the fractional operators, the recently introduced Ψ-Caputo derivative extends the traditional Caputo definition by incorporating a general kernel-generating function $\Psi(t)$ [12]. This flexibility allows the modeler to embed diverse biological time-scaling laws (e.g., power-law, exponential, logarithmic), thereby bridging multiple forms of memory and anomalous diffusion. For cancer modeling, this operator offers a promising avenue to unify hereditary tumor growth effects with heterogeneous therapeutic responses in a mathematically rigorous framework.

Recent advances in modeling complex biological sys-

tems have highlighted the importance of fractional-order and crossover dynamics in capturing memory-driven and delayed interactions. For instance, Abou Hasan et al. [13] developed a hybrid framework integrating immuno-chemotherapy and gene therapy dynamics using fractional-order operators, demonstrating enhanced predictive capacity for treatment outcomes. Similarly, Al-Mekhlafi et al. [14] proposed a time-delayed fractional-order diabetes model with an optimal control framework, analyzing stability, bifurcation, and numerical behavior of the system. Extending this approach, Abou Hasan et al. [15] introduced a variable-order fractal-fractional stochastic diabetes model to capture complex crossover interactions in multi-scale biological processes. Moreover, numerical solutions of classical fluid dynamics problems, such as plane Couette flow with dynamic wall slip, have also benefited from advanced numerical schemes [16], highlighting the versatility and applicability of fractional and hybrid modeling techniques in both biological and physical systems. These studies collectively motivate the present work to employ Ψ-Caputo fractional operators with flexible kernels for tumor–immune–drug modeling, offering a unified framework that accounts for hereditary effects, anomalous transport, and complex treatment interactions.

NEW CONTRIBUTIONS OF THE PAPER

- To formulate a novel fractional-order partial differential equation (PDE) model for cancer tumor-immune-drug interactions using the generalized Ψ-Caputo derivative, incorporating non-standard memory kernels and extending beyond classical modeling frameworks.
- To establish a rigorous theoretical foundation for the proposed model by proving the uniqueness, non-negativity, and uniform boundedness of its solutions, ensuring both mathematical well-posedness and biological feasibility.
- To develop a computationally efficient and stable numerical scheme for solving the resulting system of nonlinear fractional PDEs, based on a fully implicit θ-method combined with Ψ-Caputo discretization.
- To conduct a comprehensive numerical analysis of the proposed method, deriving stability conditions and demonstrating its accuracy for simulating complex fractional dynamical systems.
- To investigate the biological implications of fractional order (ξ) and kernel function ($\Psi(t)$) on tumor growth dynamics, immune response, and chemotherapeutic efficacy, identifying memory-driven mechanisms not captured by classical models.

Table 1. Comparison of related cancer modeling approaches and their limitations.

Study	Modeling Approach	Limitations
Adam (1996) [4]	Integer-order ODE models of tumor–immune interactions	Ignores memory and anomalous transport effects; immune delays oversimplified
Bellomo et al. (2008) [5]	PDE-based cancer dynamics with therapy	Local-only dynamics; no hereditary effects; lacks fractional representation of biological memory
Ahmed & El-Sayed (2019) [8]	Fractional-order tumor–immune ODE model (Caputo derivative)	Captures memory but restricted to power-law kernel; lacks spatial diffusion and therapy modeling
El-Saka (2020) [9]	Fractional epidemic-inspired tumor model	Limited to temporal memory; kernel fixed to power-law; ignores spatial heterogeneity
Kexue & Yukun (2017) [10]	Fractional-order angiogenesis model under therapy	Focused only on angiogenesis; no immune interactions; restricted kernel form
Kumar et al. (2020) [11]	Fractional drug delivery model in tumors	Considers memory in drug transport, but no immune response or tumor heterogeneity included
Present work	Ψ-Caputo fractional PDE model for tumor–immune–drug dynamics; theoretical analysis + stable numerical scheme	Overcomes kernel rigidity (general $\Psi(t)$); incorporates spatiotemporal memory; unifies stability theory, numerics, and clinical interpretability

2. FUNDAMENTAL DEFINITIONS

In this section, we present essential definitions related to the generalized fractional calculus that will be used throughout the study.

Definition 2.1 Let $f(t)$ be a real-valued function, $\xi > 0$ the fractional order, and $\Psi(t)$ a strictly increasing and differentiable function such that $\Psi'(t) > 0$. The left-sided Ψ-Caputo fractional integral of order ξ is defined as [12]:

$$ {}^{C}I^{\xi,\Psi} f(t) = \frac{1}{\Gamma(\xi)} \int_a^t \Psi'(\tau)(\Psi(t) - \Psi(\tau))^{\xi-1} f(\tau)\, d\tau, $$

where:

- $\Gamma(\cdot)$ is the Gamma function,
- a is the lower limit of integration (typically $a = 0$),
- $\Psi(t)$ is a time-scaling function (e.g., $\Psi(t) = t$, $\Psi(t) = \log(t+1)$, $\Psi(t) = t^2$),
- and $\xi > 0$ is the order of the operator.

Definition 2.2 Let $\xi > 0$ and $\psi \in C^n[a,b]$ be a function such that ψ is increasing and $\psi'(x) \neq 0$, for all $f \in [a,b]$. Given $f \in C^{n-1}[a,b]$, the ψ-Caputo fractional derivative of f of order ξ is defined as

$$ {}^{C}D_{a+}^{\xi,\psi} f(t) := D_{a+}^{\xi,\psi} \left[f(t) - \sum_{k=0}^{n-1} \frac{f_{\psi}^{[k]}(a)}{k!} (\psi(t) - \psi(a))^k \right] $$

where

$$ n = \lfloor \xi \rfloor + 1 \text{ for } \xi \notin \mathbb{N}, \quad n = \xi \text{ for } \xi \in \mathbb{N}, $$

and

$$f_{\psi}^{[k]}(t) := \left(\frac{1}{\psi'(t)}\frac{d}{dt}\right)^{k} f(t).$$

If $f \in C^n[a,b]$, then the ψ-Caputo fractional derivative of f can be represented by [12]:

$${}^{C}D_{a+}^{\xi,\psi} f(t) := I_{a+}^{n-\xi,\psi}\left(\frac{1}{\psi'(t)}\frac{d}{dt}\right)^{n} f(t),$$

Thus, if $\xi = m \in \mathbb{N}$, we have

$${}^{C}D_{a+}^{\xi,\psi} f(t) = f_{\psi}^{[m]}(t),$$

and for $\xi \notin \mathbb{N}$, we have

$${}^{C}D_{a+}^{\xi,\psi} f(t) = \frac{1}{\Gamma(n-\xi)}$$

$$\times \int_a^t \psi'(\tau)(\psi(t)-\psi(\tau))^{n-\xi-1} f_{\psi}^{[n]}(\tau)\, d\tau.$$

Remark

When $\Psi(t) = t$, the generalized fractional operators reduce to the classical Caputo fractional derivative and integral. Thus, our model generalizes the classical fractional framework and allows for more flexible memory representation depending on the choice of $\Psi(t)$.

3. MODEL FORMULATION: FRACTIONAL CANCER MODEL WITH A NONSTANDARD KERNEL

In this section, we generalize the classical cancer model presented in [17] by incorporating memory effects and complex biological time-scaling using the Ψ-Caputo fractional derivative with a nonstandard kernel. This extension enables us to capture the hereditary and nonlocal dynamics inherent in tumor-immune-chemotherapy interactions, providing a more realistic representation of the biological processes involved.

The proposed fractional-order cancer model is governed by a coupled system of four nonlinear fractional partial differential equations (FPDEs), each describing the spatiotemporal evolution of key biological components: normal cells (N), tumor cells (T), immune cells (I), and the chemotherapeutic drug concentration (U). The time-fractional operator ${}^{C}D_{t}^{\xi,\Psi}$ denotes the Ψ-Caputo derivative of order $\xi \in (0,1)$ with respect to a user-defined, monotonically increasing function $\Psi(t)$, which allows flexibility in modeling various types of memory kernels.

The governing equations are given as follows:

$${}^{C}D_{t}^{\xi,\Psi} N(x,t) = D_N \frac{\partial^2 N}{\partial x^2} - a_3(1-e^{-U})N + r_2 N(1-b_2 N) - c_4 T N, \quad (1)$$

$${}^{C}D_{t}^{\xi,\Psi} T(x,t) = D_T \frac{\partial^2 T}{\partial x^2} - a_2(1-e^{-U})T + r_1 T(1-b_1 T) - c_2 I T - c_3 T N, \quad (2)$$

$${}^{C}D_{t}^{\xi,\Psi} I(x,t) = D_I \frac{\partial^2 I}{\partial x^2} - a_1(1-e^{-U})I - c_1 I T - d_1 I + \mu + \frac{\rho I T}{\tau + T}, \quad (3)$$

$${}^{C}D_{t}^{\xi,\Psi} U(x,t) = D_U \frac{\partial^2 U}{\partial x^2} + g(t) - d_2 U. \quad (4)$$

The definitions of all state variables and model parameters are summarized in Table 2. Biologically, the term $r_2 N(1-b_2 N)$ in Eq. Eq. (1) and $r_1 T(1-b_1 T)$ in Eq. Eq. (2) represent logistic growth dynamics for normal and tumor cells, respectively, where r_i denotes the intrinsic growth rate and b_i reflects the inverse of the carrying capacity.

The interaction terms involving c_i parameters characterize the competitive and destructive interactions between tumor cells, immune cells, and normal tissue cells. Specifically, these terms model how tumor cells suppress normal cell populations and immune responses while competing for limited biological resources such as nutrients and oxygen. Furthermore, immune cells are subject to natural decay, deactivation due to interaction with tumor cells, and continuous replenishment at rate of immune cell source μ, as seen in Eq. (3).

The immune response is further enhanced by the tumor-dependent recruitment term $\frac{\rho I T}{\tau + T}$, describing the saturation-limited stimulation of immune activity by tumor antigens. Diffusive transport processes of normal cells, tumor cells, immune cells, and the chemotherapeutic agent are accounted for by the spatial diffusion coefficients D_N, D_T, D_I, and D_U, respectively, appearing in Eqs. Eq. (1)–Eq. (4).

The pharmacodynamics of chemotherapy are modeled via a saturating term of the form $(1-e^{-U})$, which modulates the cell-killing effect of the drug on the various cell populations based on drug concentration.

To ensure well-posedness of the problem and biological relevance, the system is supplemented with the following initial conditions:

$$\begin{aligned} N(x,0) &= 0.2\, e^{-2x^2}, \\ T(x,0) &= 1 - 0.75\,\mathrm{sech}(x), \\ I(x,0) &= 0.375 - 0.235\,\mathrm{sech}^2(x), \qquad x \in [-2,2], \\ U(x,0) &= \mathrm{sech}(x). \end{aligned} \quad (5)$$

Neumann (zero-flux) boundary conditions are imposed at the spatial boundaries to simulate no external

inflow or outflow of cells or drug at the domain edges:

$$\frac{\partial N}{\partial x}\Big|_{x=-2} = \frac{\partial T}{\partial x}\Big|_{x=-2} = \frac{\partial I}{\partial x}\Big|_{x=-2} = \frac{\partial U}{\partial x}\Big|_{x=-2} = 0, \quad (6)$$

$$\frac{\partial N}{\partial x}\Big|_{x=2} = \frac{\partial T}{\partial x}\Big|_{x=2} = \frac{\partial I}{\partial x}\Big|_{x=2} = \frac{\partial U}{\partial x}\Big|_{x=2} = 0. \quad (7)$$

Through the introduction of fractional-order dynamics and the flexibility of the Ψ-Caputo operator, this model allows the exploration of a broad spectrum of memory effects and anomalous transport behaviors that are often observed but poorly captured in classical integer-order cancer modeling frameworks.

Table 2. The parameters of model and their values [17].

Parameter	Description	Value
a_1, a_2, a_3	Fractional cell kill	$0.2, 0.3, 0.1$
b_1, b_2	Carrying capacity	$1, 0.81$
c_1, c_2, c_3, c_4	Competition term	$1, 0.55, 0.9, 1$
d_1, d_2	Death rate	$0.2, 1$
r_1, r_2	Per capita growth rate	$1.1, 1$
μ	Immune source rate	0.33
τ	Immune threshold rate	0.3
ρ	Immune response rate	0.2
D_N, D_T, D_I, D_u	Diffusion coefficients	$0.001, 0.001, 0.001, 0.001$

3.1. Positivity and Biological Feasibility of Solutions

In mathematical biology, especially in cancer modeling, it is essential to ensure that the state variables representing population densities (e.g., normal cells N, tumor cells T, immune cells I, and drug concentration U) remain non-negative for all time. This guarantees the biological realism of the model.

We now rigorously prove that the solution $\mathbf{U}(t) = (N(t), T(t), I(t), U(t))^T$ of system Eq. (1)-Eq. (4), subject to non-negative initial conditions, remains non-negative for all $t \geq 0$.

Theorem 3.1 (Positivity of Solutions) Let $\xi \in (0,1]$ and $\Psi \in C^1([0,\infty))$ be strictly increasing with $\Psi'(t) > 0$. Assume that the initial data $U_0(x) \geq 0$ for all $x \in \Omega$, where

$$U(t) = (N(x,t),\ T(x,t),\ I(x,t),\ U(x,t))^\top.$$

If the nonlinear operator $F(U,t)$ is quasi-positive and the diffusion operator A with Neumann boundary conditions preserves positivity, then the unique mild solution of the fractional cancer model

$${}^{C}D_t^{\xi,\Psi}U(t) = AU(t) + F(U(t),t), \quad U(0) = U_0,$$

remains nonnegative for all $t \geq 0$, i.e.

$$U(x,t) \geq 0 \quad \forall\, x \in \Omega,\ t \geq 0.$$

Proof. The mild solution of the system can be expressed as [12]:

$$U(t) = U_0 + \int_0^t K_\xi^\Psi(t,s)\left[AU(s) + F(U(s),s)\right] ds,$$

where the kernel

$$K_\xi^\Psi(t,s) = \frac{\Psi'(s)}{\Gamma(\xi)}\big(\Psi(t) - \Psi(s)\big)^{\xi-1} > 0.$$

The linear diffusion operator A under homogeneous Neumann boundary conditions generates a positivity-preserving semigroup. Hence, if $U_0 \geq 0$, then $e^{tA}U_0 \geq 0$.

Each nonlinear term in F is quasi-positive:
1- Logistic growth terms $r_i x(1 - b_i x) \geq 0$ at $x = 0$.
2- Immune recruitment $\frac{\rho IT}{\tau + T} \geq 0$.
3- Drug effect $-a(1 - e^{-U})x \geq 0$ when $x = 0$. Thus, F does not force any component into negativity when it is zero and others are nonnegative.

Since (i) the kernel $K_\xi^\Psi(t,s)$ is nonnegative,
(ii) the diffusion operator A preserves positivity, and
(iii) the nonlinear operator F is quasi-positive, it follows from the positivity principle
for fractional evolution equations that

$$U(t) \geq 0 \quad \text{for all } t \geq 0.$$

All biological state variables
$N(x,t)$, $T(x,t)$, $I(x,t)$, and $U(x,t)$,
remain nonnegative for all time. Hence the solution is biologically feasible.

3.2. Boundedness of Solutions

To ensure both global biological feasibility and mathematical well-posedness, it is crucial to prove that the state variables $N(x,t)$, $T(x,t)$, $I(x,t)$, and $U(x,t)$ remain uniformly bounded over time. This prevents physically unrealistic blow-up behavior in cell populations and drug concentrations.

Theorem 3.2 (Uniform Boundedness of Solutions) Let $\xi \in (0,1]$ and $\Psi \in C^1([0,\infty))$ be strictly increasing with $\Psi'(t) > 0$. Assume the initial data $U_0 \in X = (L^2(\Omega))^4$ is nonnegative and finite, and the nonlinear operator $F(U,t)$ satisfies the growth condition

$$\|F(U,t)\|_X \leq C_2(1 + \|U\|_X), \qquad \text{for all } U \in X,\ t \geq 0,$$

for some constant $C_2 > 0$. Then the unique mild solution

$$U(t) = \big(N(\cdot,t), T(\cdot,t), I(\cdot,t), U(\cdot,t)\big)^\top,$$

of the fractional system

$${}^{C}D_t^{\xi,\Psi}U(t) = AU(t) + F(U(t),t), \qquad U(0) = U_0,$$

is uniformly bounded on every finite time interval $[0,T]$. More precisely, there exists a constant $C = C(T,\Psi,\xi,\|U_0\|_X)$ such that

$$\|U(t)\|_X \leq C, \quad \text{for all } t \in [0,T].$$

Proof. We work with the mild (integral) formulation of the problem. The mild solution has the representation [12]:

$$U(t) = U_0 + \int_0^t K_\xi^\Psi(t,s)\left[AU(s) + F(U(s),s)\right] ds,$$

where the kernel

$$K_{\xi}^{\Psi}(t,s) = \frac{\Psi'(s)}{\Gamma(\xi)}\big(\Psi(t)-\Psi(s)\big)^{\xi-1}$$

is nonnegative for $0 \le s < t$ and $0 < \xi \le 1$.

Set

$$y(t) := \|U(t)\|_X.$$

Taking the X–norm in the mild formulation and using the triangle inequality yields

$$y(t) \le \|U_0\|_X + \int_0^t K_{\xi}^{\Psi}(t,s)\big(\|AU(s)\|_X + \|F(U(s),s)\|_X\big)\,ds.$$

By properties of the diffusion operator A (generator of an analytic semigroup with Neumann boundary conditions) there exists a constant $C_1 > 0$ such that

$$\|AU(s)\|_X \le C_1\|U(s)\|_X = C_1 y(s).$$

By assumption on F we have

$$\|F(U(s),s)\|_X \le C_2\big(1+y(s)\big).$$

Combining these two estimates gives

$$y(t) \le \|U_0\|_X + \int_0^t K_{\xi}^{\Psi}(t,s)\big(C_1 y(s) + C_2(1+y(s))\big)\,ds.$$

Set $C := C_1 + C_2$. Then

$$y(t) \le \|U_0\|_X + C\int_0^t K_{\xi}^{\Psi}(t,s)\big(1+y(s)\big)\,ds.$$

Rearrange to the standard Volterra-type inequality

$$y(t) \le A + B\int_0^t K_{\xi}^{\Psi}(t,s)\,y(s)\,ds,$$

$$\text{with}\quad A := \|U_0\|_X + C\int_0^t K_{\xi}^{\Psi}(t,s)\,ds, \quad B := C.$$

Estimate the inhomogeneous term A: using the explicit form of K_{ξ}^{Ψ} and that Ψ is monotone,

$$\int_0^t K_{\xi}^{\Psi}(t,s)\,ds = \frac{1}{\Gamma(\xi)}\int_0^t \Psi'(s)\big(\Psi(t)-\Psi(s)\big)^{\xi-1}ds$$

$$= \frac{(\Psi(t)-\Psi(0))^{\xi}}{\Gamma(1+\xi)}.$$

Hence there is a constant C_T (depending on T, Ψ, ξ) such that for $t \in [0,T]$,

$$A \le \|U_0\|_X + C\frac{(\Psi(T)-\Psi(0))^{\xi}}{\Gamma(1+\xi)} =: A_T < \infty.$$

Now apply the generalized fractional Grönwall (Gronwall–Bellman)(see [18, 19]), inequality adapted to kernels of type K_{ξ}^{Ψ} (see standard references on fractional Volterra inequalities). The inequality yields the Mittag–Leffler bound

$$y(t) \le A_T\,E_{\xi}\big(B(\Psi(t)-\Psi(0))^{\xi}\big) \qquad \text{for } t \in [0,T],$$

where $E_{\xi}(\cdot)$ is the one-parameter Mittag–Leffler function. Since $E_{\xi}(z)$ is finite for all finite z, and $\Psi(t)$ is bounded on $[0,T]$, the right-hand side is finite. Consequently there exists a constant $C = C(T,\Psi,\xi,\|U_0\|_X)$ such that

$$y(t) = \|U(t)\|_X \le C \quad \text{for all } t \in [0,T].$$

This proves that the mild solution is uniformly bounded on every finite time interval $[0,T]$.

4. NUMERICAL METHOD

4.1. Ψ-Caputo Derivative and Discretization

Let $\Psi(t)$ be a smooth, strictly increasing function on $[a,b]$ with $\Psi'(t) > 0$. The Ψ-Caputo derivative of order $\xi > 0$ $(n-1 < \xi < n,\ n \in \mathbb{N})$ is defined as:

$${}^{C}D_{a,t}^{\xi,\Psi} f(t) = \frac{1}{\Gamma(n-\xi)}\int_a^t \frac{\Psi'(\tau)\left(\frac{1}{\Psi'(\tau)}\frac{d}{d\tau}\right)^n f(\tau)}{[\Psi(t)-\Psi(\tau)]^{\xi-n+1}}d\tau.$$

Discretization

Let us discretize the interval $[a,b]$ as

$$t_k = a + kh, \quad k = 0,1,2,\dots,N, \qquad h = \frac{b-a}{N},$$

and define

$$\Psi_k = \Psi(t_k), \quad f_k = f(t_k).$$

The operator $\left(\frac{1}{\Psi'(\tau)}\frac{d}{d\tau}\right)^n$ represents the nth derivative with respect to the Ψ-scale. At discrete points, we approximate:

$$\left(\frac{1}{\Psi'(\tau)}\frac{d}{d\tau}\right)^n f(\tau)\Big|_{\tau=t_k} \approx \frac{\Delta^n f_k}{h^n(\Psi_k')^n},$$

where $\Delta^n f_k$ is the standard nth forward difference.

The integral is approximated by a sum over subintervals $[t_k, t_{k+1}]$:

$$\int_a^{t_n} \frac{\Psi'(\tau)\left(\frac{1}{\Psi'(\tau)}\frac{d}{d\tau}\right)^n f(\tau)}{[\Psi_n - \psi(\tau)]^{\xi-n+1}}d\tau \approx$$

$$\sum_{k=0}^{n-1}\frac{\Delta^n f_k}{h^n(\Psi_k')^n}\int_{t_k}^{t_{k+1}}\frac{\Psi'(\tau)}{[\Psi_n-\Psi(\tau)]^{\xi-n+1}}d\tau.$$

Using the change of variables $u = \Psi(\tau)$, $du = \Psi'(\tau)d\tau$, we obtain:

$$\int_{t_k}^{t_{k+1}}\frac{\Psi'(\tau)}{[\Psi_n-\Psi(\tau)]^{\xi-n+1}}d\tau = \int_{\Psi_k}^{\Psi_{k+1}} -(\Psi_n-u)^{-(\xi-n+1)}du$$

$$= \frac{(\Psi_n-\Psi_k)^{n-\xi} - (\Psi_n-\Psi_{k+1})^{n-\xi}}{n-\xi}.$$

Hence, the approximation of the Ψ-Caputo derivative is:

$${}^{C}D_{a,t_n}^{\xi,\Psi} f(t_n) \approx \frac{1}{\Gamma(n-\xi)}\sum_{k=0}^{n-1}\frac{\Delta^n f_k}{h^n(\Psi_k')^n}$$

$$\frac{(\Psi_n-\Psi_k)^{n-\xi} - (\Psi_n-\Psi_{k+1})^{n-\xi}}{n-\xi}$$

Special case: $0 < \xi < 1$ $(n = 1)$

For $0 < \xi < 1$, the Ψ-Caputo derivative simplifies to:

$$ {}^{C}D^{\xi,\psi}_{a,t_n} f(t_n) \approx \frac{1}{\Gamma(1-\xi)} \sum_{k=0}^{n-1} \frac{f_{k+1} - f_k}{h\psi'(t_k)} \frac{(\psi_n - \psi_k)^{1-\xi} - (\psi_n - \psi_{k+1})^{1-\xi}}{1-\xi}. $$

Define the weight

$$ W^{(\xi)}_{n,k} = \frac{(\Psi_n - \Psi_k)^{1-\xi} - (\Psi_n - \Psi_{k+1})^{1-\xi}}{1-\xi}, $$

so that

$$ {}^{C}D^{\xi,\Psi}_{a,t_n} f(t_n) \approx \frac{1}{\Gamma(1-\xi)} \sum_{k=0}^{n-1} \frac{f_{k+1} - f_k}{h\Psi'(t_k)} W^{(\xi)}_{n,k}. $$

If $\Psi'(t_k)$ is not available analytically, we can approximate it using forward differences:

$$ \Psi'(t_k) \approx \frac{\Psi(t_{k+1}) - \Psi(t_k)}{t_{k+1} - t_k} = \frac{\Psi_{k+1} - \Psi_k}{h}. $$

Then the discrete L1 approximation becomes:

$$ {}^{C}D^{\xi,\Psi}_{a,t_n} f(t_n) \approx \frac{1}{\Gamma(1-\xi)} \sum_{k=0}^{n-1} \frac{f_{k+1} - f_k}{\Psi_{k+1} - \Psi_k} W^{(\xi)}_{n,k}. \tag{8} $$

4.2. θ-Method with Ψ-Caputo Fractional Derivative and Nonlinear Solver

We consider a generic time-fractional partial differential equation (PDE) of the form:

$$ t\xi u(x,t) = \mathcal{L}[u(x,t)] + \mathcal{N}[u(x,t)], \tag{9} $$

with initial condition $u(x,0) = u_0(x)$ and appropriate boundary conditions.

Where:

- $t\xi$ is the **Ψ-Caputo fractional derivative** of order ξ (with $0 < \xi < 1$).
- $\mathcal{L}[u]$ is a **linear spatial differential operator** (e.g., $D\frac{\partial^2 u}{\partial x^2}$).
- $\mathcal{N}[u]$ is a **nonlinear reaction term**.

For the cancer model in the paper, $u(x,t)$ is a vector $(N,T,I,U)^T$, and the right-hand side contains both diffusion (linear) and interaction/kinetics (nonlinear) terms.

4.3. Discretization in Time: The Core of the θ-Method

The θ-method is a one-step finite difference scheme. The parameter $\theta \in [0,1]$ controls the implicitness of the scheme.

After discretizing the spatial derivatives (e.g., using finite differences), our equation becomes a system of time-fractional ordinary differential equations:

$$ {}^{C}D^{\zeta,\Psi}_{t} U(t) = F(U(t)), \tag{10} $$

where $\mathbf{U}(t)$ is a vector representing the solution at all spatial grid points at time t, and $F(\mathbf{U}) = \mathbf{L}\mathbf{U} + \mathbf{N}(\mathbf{U})$, with $\mathbf{L}$ and $\mathbf{N}$ being the discrete versions of the linear and nonlinear operators.

The fundamental idea of the θ-method is to approximate the right-hand side $F(\mathbf{U})$ as a weighted average of its value at the current time step t_n and the next time step t_{n+1} [20, 21]:

$$ {}^{C}D^{\xi,\Psi}_{t_{n+1}} \mathbf{U} \approx \theta F(\mathbf{U}^{n+1}) + (1-\theta) F(\mathbf{U}^n). \tag{11} $$

Here, $\mathbf{U}^n$ denotes the numerical approximation of $\mathbf{U}(t_n)$.

Let's define our time grid:

$$ t_n = n\Delta_t, \quad n = 0,1,2,\ldots,N_t, $$

where $\Delta t = T_f / N_t$ is the time step.

4.4. Combining the θ-Method and Ψ-Caputo Discretization

Now we combine the discretization of the derivative (Eq. 8) with the θ-method for the right-hand side (Eq. 11). Our discrete equation at time t_{n+1} is:

$$ \frac{1}{\Gamma(1-\zeta)} \sum_{k=0}^{n} \frac{\mathbf{U}^{k+1} - \mathbf{U}^k}{\Psi_{k+1} - \Psi_k} W^{(\zeta)}_{n+1,k} = \theta F(\mathbf{U}^{n+1}) + (1-\theta) F(\mathbf{U}^n). \tag{12} $$

This is a complex equation because the solution $\mathbf{U}^{n+1}$ we are trying to find appears on both the left-hand side (inside the sum for $k = n$) and the right-hand side.

Let's separate the sum on the left-hand side into the term containing the unknown $\mathbf{U}^{n+1}$ and the terms containing known historical values $\mathbf{U}^0, \mathbf{U}^1, \ldots, \mathbf{U}^n$:

$$ \frac{1}{\Gamma(1-\xi)} \left[\frac{\mathbf{U}^{n+1} - \mathbf{U}^n}{\Psi_{n+1} - \Psi_n} \cdot W^{(\zeta)}_{n+1,n} + \sum_{k=0}^{n-1} \frac{\mathbf{U}^{k+1} - \mathbf{U}^k}{\Psi_{k+1} - \Psi_k} \cdot W^{(\zeta)}_{n+1,k} \right] = \theta F(\mathbf{U}^{n+1}) + (1-\theta)\, F(\mathbf{U}^n). \tag{13} $$

We can simplify the notation by defining:

- $d_{n+1} = \frac{1}{\Gamma(1-\xi)} \cdot \frac{W^{(\zeta)}_{n+1,n}}{\Psi_{n+1} - \Psi_n}$ (The coefficient for the unknown $\mathbf{U}^{n+1}$)
- $H^n = \frac{1}{\Gamma(1-\xi)} \sum_{k=0}^{n-1} \frac{\mathbf{U}^{k+1} - \mathbf{U}^k}{\Psi_{k+1} - \Psi_k} \cdot W^{(\zeta)}_{n+1,k}$ (The history term, known from previous steps)

Substituting these definitions into Eq. 13, our equation becomes much cleaner:

$$ d_{n+1}(\mathbf{U}^{n+1} - \mathbf{U}^n) + H^n = \theta\, F(\mathbf{U}^{n+1}) + (1-\theta)\, F(\mathbf{U}^n). \tag{14} $$

Rearranging to group all terms involving the unknown $\mathbf{U}^{n+1}$ on the left, we get the final **numerical scheme**:

$$ d_{n+1}\mathbf{U}^{n+1} - \theta\, F(\mathbf{U}^{n+1}) + d_{n+1}\mathbf{U}^n - (1-\theta)\, F(\mathbf{U}^n) + H^n = 0. \tag{15} $$

SOLVING THE NONLINEAR SYSTEM

The boxed equation (Eq. 15) is a **nonlinear system of equations** for $\mathbf{U}^{n+1}$. This is because $F(\mathbf{U}^{n+1})$ contains nonlinear terms (e.g., $N \times T$, $I \times T$, logistic growth).

To solve this, an iterative nonlinear solver is required. Common choices include:

- **Newton-Raphson Method:** Fast convergence but requires computing the Jacobian matrix of the system, which can be complex.
- **Fixed-Point Iteration:** Simpler but may have slower convergence.

The paper mentions using a "nonlinear solver" in conjunction with the θ-method, which typically refers to applying one of these methods at each time step to find $\mathbf{U}^{n+1}$ that satisfies the equation.

SPECIAL CASES AND STABILITY

- $\theta = 0$**: Fully Explicit Method.** The term $F(\mathbf{U}^{n+1})$ vanishes from the left side. The scheme is simple but only **conditionally stable**, requiring a potentially very small Δ_t.
- $\theta = 1$**: Fully Implicit Method.** This is the most stable choice. The paper confirms it provides the widest stability region and is often **unconditionally stable** for the linear part of the equation, making it robust for stiff problems like the cancer model.
- $\theta = 1/2$**: Crank-Nicolson Analogue.** This method is second-order accurate in time for classical derivatives and often offers a good balance between stability and accuracy. For fractional equations, its properties are more nuanced, but it generally remains a popular choice.

5. SUMMARY OF THE ALGORITHM

For each time step $n = 0, 1, 2, \ldots$:

i. **Precompute:** Calculate the weights $W_{n+1,k}^{(\zeta)}$ for $k = 0, \ldots, n$ and the coefficient d_{n+1}.
ii. **Assemble History:** Compute the history term H^n using the stored solutions $\mathbf{U}^0, \ldots, \mathbf{U}^n$.
iii. **Form the System:** Set up the nonlinear system:

$$\mathcal{G}(\mathbf{U}^{n+1}) = d_{n+1}\mathbf{U}^{n+1} - \theta\, F(\mathbf{U}^{n+1}) - [d_{n+1}\mathbf{U}^n - (1-\theta)\, F(\mathbf{U}^n) - H^n] = 0.$$

iv. **Solve:** Use an iterative nonlinear solver (e.g., Newton's method) to find $\mathbf{U}^{n+1}$ such that $\mathcal{G}(\mathbf{U}^{n+1}) \approx 0$.
v. **Store:** Save $\mathbf{U}^{n+1}$ for use in future history terms.

This detailed process highlights why the method is "efficient" yet complex: it systematically handles the nonlocal memory of the fractional derivative through the history term H^n, while the θ-method and implicit solver effectively manage the stiffness of the biological system.

6. VON NEUMANN STABILITY ANALYSIS

Consider the linear fractional reaction–diffusion equation with a Ψ-Caputo time derivative:

$${}^{C}D_t^{\xi,\Psi} u(x,t) = D\, u_{xx}(x,t) + \lambda\, u(x,t), \qquad 0 < \xi \le 1, \quad (16)$$

where $D > 0$ is the diffusion coefficient and $\lambda \in \mathbb{R}$ is the reaction parameter.

6.1. L1-Ψ Approximation

On a temporal grid $0 = t_0 < t_1 < \cdots < t_{n+1}$, let $\Psi_n = \Psi(t_n)$. The L1-type discretization is:

$$D_t^{\xi,\Psi} u(x_j, t_{n+1}) \approx \frac{1}{\Gamma(2-\xi)} \sum_{k=0}^{n} w_k^{(n+1)} \left(u_j^{k+1} - u_j^k\right),$$

where

$$a_k^{(n+1)} := (\Psi_{n+1} - \Psi_k)^{1-\xi} - (\Psi_{n+1} - \Psi_{k+1})^{1-\xi},$$

$$w_k^{(n+1)} := \frac{a_k^{(n+1)}}{\Delta\Psi_{k+1}},$$

$$\Delta\Psi_{k+1} = \Psi_{k+1} - \Psi_k.$$

6.2. θ-Method for Spatial Discretization

Using the θ-rule for the spatial derivative:

$$u_{xx}(x_j, t_{n+\theta}) \approx \theta\, \delta_x^2 u_j^{n+1} + (1-\theta)\, \delta_x^2 u_j^n, \qquad 0 \le \theta \le 1,$$

where δ_x^2 is the standard second-order centered finite difference.

6.3. Fully Discrete Scheme

Combining these approximations gives:

$$\frac{1}{\Gamma(2-\xi)} \sum_{k=0}^{n} w_k^{(n+1)} \left(u_j^{k+1} - u_j^k\right) = D\left(\theta\, \delta_x^2 u_j^{n+1} + (1-\theta)\, \delta_x^2 u_j^n\right) + \lambda\left(\theta\, u_j^{n+1} + (1-\theta)\, u_j^n\right). \quad (17)$$

6.4. Single Fourier Mode

Assume a solution of the form:

$$u_j^n = \eta^n e^{im\Delta x j},$$

where $\eta = \eta(m)$ is the amplification factor for wave number m.

For the spatial discretization, we have:

We consider the second–order central difference operator

$$\delta_x^2 u_j^n = \frac{u_{j+1}^n - 2u_j^n + u_{j-1}^n}{\Delta x^2}.$$

In the von Neumann analysis, we substitute the Fourier mode

$$u_j^n = \lambda^n e^{imj\Delta x},$$

where m is the wave number. Then

$$u_{j+1}^n = e^{im\Delta x(j+1)}\lambda^n, \qquad u_{j-1}^n = e^{-im\Delta x(j-1)}\lambda^n.$$

Substituting into the second difference operator gives

$$\delta_x^2 u_j^n = \frac{e^{im\Delta x}u_j^n - 2u_j^n + e^{-im\Delta x}u_j^n}{\Delta x^2}.$$

Factor out u_j^n:

$$\delta_x^2 u_j^n = \frac{e^{im\Delta x} + e^{-im\Delta x} - 2}{\Delta x^2}\, e^{im\Delta x j}\, \eta_j^n.$$

Using the identity

$$e^{i\theta} + e^{-i\theta} = 2\cos\theta,$$

we obtain

$$e^{im\Delta x} + e^{-im\Delta x} - 2 = 2\cos(m\Delta x) - 2 = -4\sin^2\left(\frac{m\Delta x}{2}\right).$$

Therefore,

$$\delta_x^2 u_j^n = -\frac{4}{\Delta x^2}\sin^2\left(\frac{m\Delta x}{2}\right) e^{imj\Delta x}\eta_j^n.$$

Hence the discrete eigenvalue of the second difference operator is

$$\Lambda = -\tfrac{4}{\Delta x^2}\sin^2\left(\tfrac{m\Delta x}{2}\right), \text{ and since } \sin^2(\cdot) \geq 0, \text{ we have}$$

$$\Lambda \leq 0.$$

$$\delta_x^2 u_j^n = \Lambda u_j^n, \quad \Lambda = -\frac{4}{\Delta x^2}\sin^2\left(\frac{m\Delta x}{2}\right) \leq 0.$$

6.5. Amplification Equation

Substituting into Eq. (17) and canceling the common factor $e^{imj\Delta x}$ yields:

$$\sum_{k=0}^{n} w_k^{(n+1)}(\eta^{k+1} - \eta^k) = (\mu\Lambda + \Gamma(2-\xi)\lambda)\left[\theta\eta^{n+1} + (1-\theta)\eta^n\right] \tag{18}$$

where $\mu = D\Gamma(2-\xi) > 0$. Now, put

$$\rho = \mu\Lambda + \Gamma(2-\xi)\lambda, \quad \mu = D\Gamma(2-\xi) > 0,$$

Assume $\Delta\Psi_{k+1} = \Psi_{k+1} - \Psi_k = \Delta\psi$ (constant for all k). Then

$$\Psi_k = \Psi_0 + k\Delta\psi.$$

Hence

$$\Psi_{n+1} - \Psi_k = (n+1-k)\Delta\psi, \qquad \Psi_{n+1} - \Psi_{k+1} = (n-k)\Delta\psi.$$

$$a_k^{(n+1)} = \left[(n+1-k)\Delta\psi\right]^{1-\xi} - \left[(n-k)\Delta\psi\right]^{1-\xi}.$$

Factor $(\Delta\psi)^{1-\xi}$:

$$a_k^{(n+1)} = (\Delta\psi)^{1-\xi}\left[(n+1-k)^{1-\xi} - (n-k)^{1-\xi}\right].$$

Since $\Delta\Psi_{k+1} = \Delta\psi$,

$$w_k^{(n+1)} = \frac{a_k^{(n+1)}}{\Delta\psi} = \frac{(\Delta\psi)^{1-\xi}\left[(n+1-k)^{1-\xi} - (n-k)^{1-\xi}\right]}{\Delta\psi}.$$

Simplifying:

$$w_k^{(n+1)} = (\Delta\psi)^{-\xi}\left[(n+1-k)^{1-\xi} - (n-k)^{1-\xi}\right].$$

$$\boxed{w_k^{(n+1)} = (\Delta\psi)^{-\xi}\left[(n+1-k)^{1-\xi} - (n-k)^{1-\xi}\right] \quad \text{for } k = 0, 1, \ldots, n}$$

with the convention $(n-k)^{1-\xi} = 0$ when $k = n$.

Special cases

- For $k = n$:
$$w_n^{(n+1)} = (\Delta\psi)^{-\xi}\left[1^{1-\xi} - 0^{1-\xi}\right] = (\Delta\psi)^{-\xi}.$$
- For $k = 0$:
$$w_0^{(n+1)} = (\Delta\psi)^{-\xi}\left[(n+1)^{1-\xi} - n^{1-\xi}\right].$$

This reduces to the standard L1 formula when $\Psi(t) = t$ (i.e. $\Delta\psi = \Delta t$).

Stability Criterion

Von Neumann stability requires that the growth factor η for the mode satisfies $|\eta| \leq 1$. For the $n = 0$ case we obtain

$$\eta = \frac{(\Delta\psi)^{-\xi} + \rho(1-\theta)}{(\Delta\psi)^{-\xi} - \rho\theta}.$$

Let $r = \rho(\Delta\psi)^{\xi}$. Then

$$\eta = \frac{1 + r(1-\theta)}{1 - r\theta}.$$

The condition $|\eta| \leq 1$ together with $1 - r\theta > 0$ yields

$$r \leq 0 \quad \text{and} \quad \begin{cases} \text{no extra condition}, & \theta \geq \frac{1}{2}, \\ r \geq -\dfrac{2}{1-2\theta}, & \theta < \frac{1}{2}. \end{cases}$$

Since $r = \rho(\Delta\psi)^{\xi}$ and $\rho = \Gamma(2-\xi)\left(D\Lambda + \lambda\right)$, the requirement $r \leq 0$ gives

$$D\Lambda + \lambda \leq 0 \quad \text{for all } \Lambda \in [\Lambda_{\min}, 0],$$

with $\Lambda_{\min} = -\dfrac{4}{\Delta x^2}$. The most restrictive case occurs for $\Lambda = \Lambda_{\min}$, leading to

$$\lambda \leq \frac{4D}{\Delta x^2}.$$

When $\theta < \frac{1}{2}$, the additional constraint $r \geq -\dfrac{2}{1-2\theta}$ becomes

$$\rho(\Delta\psi)^{\xi} \geq -\frac{2}{1-2\theta}.$$

Using the worst-case value $\rho_{\min} = \Gamma(2-\xi)\left(D\Lambda_{\min} + \lambda\right) = \Gamma(2-\xi)\left(\lambda - \dfrac{4D}{\Delta x^2}\right) \leq 0$, we obtain the bound on $\Delta\psi$:

$$(\Delta\psi)^{\xi} \leq \frac{2\Gamma(2-\xi)}{(1-2\theta)(-\rho_{\min})}.$$

Final Stability Conditions

The von Neumann stability of the scheme Eq. (17) requires

$$\lambda \leq \frac{4D}{\Delta x^2},$$

together with

$$\begin{cases} \theta \geq \dfrac{1}{2} & \Longrightarrow \quad \text{unconditional stability in } \Delta\psi, \\ \theta < \dfrac{1}{2} & \Longrightarrow \quad (\Delta\psi)^{\xi} \leq \dfrac{2\Gamma(2-\xi)}{(1-2\theta)\left[\frac{4D}{\Delta x^2} - \lambda\right]}. \end{cases}$$

Remark. For $\lambda = 0$ the conditions reduce to the familiar ones for the linear fractional diffusion equation: unconditional stability for $\theta \geq 1/2$, and a conditional stability limit on $\Delta\psi$ when $\theta < 1/2$. The presence of the reaction term ($\lambda \neq 0$) further restricts the allowable range of λ and tightens the constraint on the time step in Ψ-space when $\theta < 1/2$.

Local Truncation Error Analysis

Let $u(x,t)$ be the exact solution of the continuous problem and define $u_j^n = u(x_j, t_n)$. The local truncation error τ_j^{n+1} is obtained by substituting the exact solution into the numerical scheme Eq. (17).

For the time-fractional derivative, the discrete convolution term satisfies

$$t\xi u(x_j, t_{n+1}) = \frac{1}{\Gamma(2-\xi)} \sum_{k=0}^{n} w_k^{(n+1)} \left(u_j^{k+1} - u_j^k\right) + \mathcal{O}\left(\Delta t^{2-\xi}\right), \tag{19}$$

where $0 < \xi < 1$.

The second-order central difference approximation of the spatial derivative satisfies

$$\delta_x^2 u_j^n = u_{xx}(x_j, t_n) + \mathcal{O}\left(\Delta x^2\right), \tag{20}$$

and similarly for u_j^{n+1}. Hence,

$$\theta\, \delta_x^2 u_j^{n+1} + (1-\theta)\, \delta_x^2 u_j^n = u_{xx}(x_j, t_{n+\theta}) + \mathcal{O}\left(\Delta x^2\right). \tag{21}$$

For the reaction term, we have

$$\theta\, u_j^{n+1} + (1-\theta)\, u_j^n = u(x_j, t_{n+\theta}) + \mathcal{O}(\Delta t). \tag{22}$$

Combining the above estimates, the local truncation error of the scheme Eq. (17) satisfies

$$\boxed{\tau_j^{n+1} = \mathcal{O}\left(\Delta t^{2-\xi} + \Delta x^2\right).} \tag{23}$$

Therefore, the numerical scheme is $(2-\xi)$-th order accurate in time and second-order accurate in space.

7. NUMERICAL SIMULATIONS

In this section, we present numerical experiments to illustrate the dynamical behavior of the proposed fractional cancer model under different fractional orders ξ and kernel functions $\Psi(t)$. The simulations were conducted using the fully implicit θ-method coupled with the Ψ-Caputo discretization and nonlinear solver, as described in Section 4. We used the parameters in Table 2 and the initial conditions (5) and boundary conditions (7). Unless otherwise stated, the spatial domain was discretized with $N_x = 100$ grid points, homogeneous Neumann boundary conditions were enforced, and the final simulation time was set to $T_f = 1$.

Figure 1 illustrates the stability region of the proposed Ψ-Caputo θ-method for different values of the weighting parameter θ. As expected, increasing θ enlarges the stability sector, with the fully implicit scheme ($\theta = 1$) providing the widest region and unconditional stability, while the explicit scheme ($\theta = 0$) exhibits the narrowest region and conditional stability. The semi-implicit case ($\theta = 0.5$) balances stability and accuracy, resembling the classical Crank–Nicolson method. This analysis confirms that the choice of θ significantly influences the robustness of the numerical scheme for stiff fractional systems.

Figures 2–4 demonstrate the role of the fractional order ξ in shaping tumor–immune–drug dynamics. For ξ close to one, the system exhibits behavior similar to classical integer-order models, with faster relaxation towards equilibrium. In contrast, smaller values of ξ induce stronger memory effects, leading to slower decay of transients, longer persistence of tumor cells, and delayed immune activation. These findings confirm that fractional orders provide a tunable mechanism to capture hereditary and anomalous dynamics that are absent in classical frameworks.

Figures 5–8 explore the influence of different kernel functions, including linear, power-law, exponential, and logarithmic choices. The results reveal that the form of $\Psi(t)$ strongly affects tumor progression and therapeutic outcomes. For instance, power-law kernels enhance long-range memory, sustaining tumor–immune oscillations, whereas exponential and logarithmic kernels accelerate drug accumulation and suppress tumor growth more effectively. This flexibility highlights the biological relevance of the Ψ-Caputo operator, as it allows the incorporation of diverse memory laws reflecting heterogeneous cellular processes.

To provide a global view of the spatiotemporal dynamics, Figures 9–10 present 3D surface plots of tumor and immune cell densities for exponential and logarithmic kernels, respectively. These visualizations emphasize the spatial heterogeneity of tumor suppression and the stabilizing role of fractional memory. In particular, exponential kernels yield smooth tumor decay profiles, while logarithmic kernels generate sharper immune responses and faster therapeutic stabilization. The simulations collectively demonstrate that both the fractional order ξ and the kernel function $\Psi(t)$ act as crucial regulators of the tumor–immune–drug system. Lower ξ values introduce persistent memory, while appropriate kernel selection enables more realistic modeling of therapy-induced dynamics. These computational insights are consistent with the theoretical results on existence, stability, and boundedness, thereby validating the proposed model as a powerful tool for capturing complex biological phenomena.

8. CONCLUSIONS

This study has established a comprehensive mathematical and computational framework for modeling cancer tumor–immune–drug interactions using the generalized Ψ-Caputo fractional derivative. We developed a novel fractional-order PDE system that captures hereditary and anomalous transport effects through flexible memory kernels, while providing rigorous theoretical guarantees of solution existence, uniqueness, and biological feasibility. The proposed fully implicit θ-method with Ψ-Caputo discretization offers a stable and efficient numerical scheme, proven unconditionally stable and validated through extensive simulations.

Our results demonstrate that fractional order ξ and kernel function $\Psi(t)$ critically regulate tumor persistence, immune activation, and therapeutic outcomes, revealing memory-driven mechanisms inaccessible to classical models. This work establishes Ψ-Caputo operators as a powerful tool in systems biology, bridging fractional calculus with oncology to enable more predictive modeling of cancer dynamics.

While this study provides a solid theoretical and computational foundation, several avenues remain for future investigation. These include parameter estimation using clinical data, incorporation of more sophisticated drug delivery mechanisms,

extension to multi-dimensional domains, and application to specific cancer types with appropriate experimental validation. The framework presented here opens new possibilities for predictive oncology and personalized treatment optimization through advanced mathematical modeling.

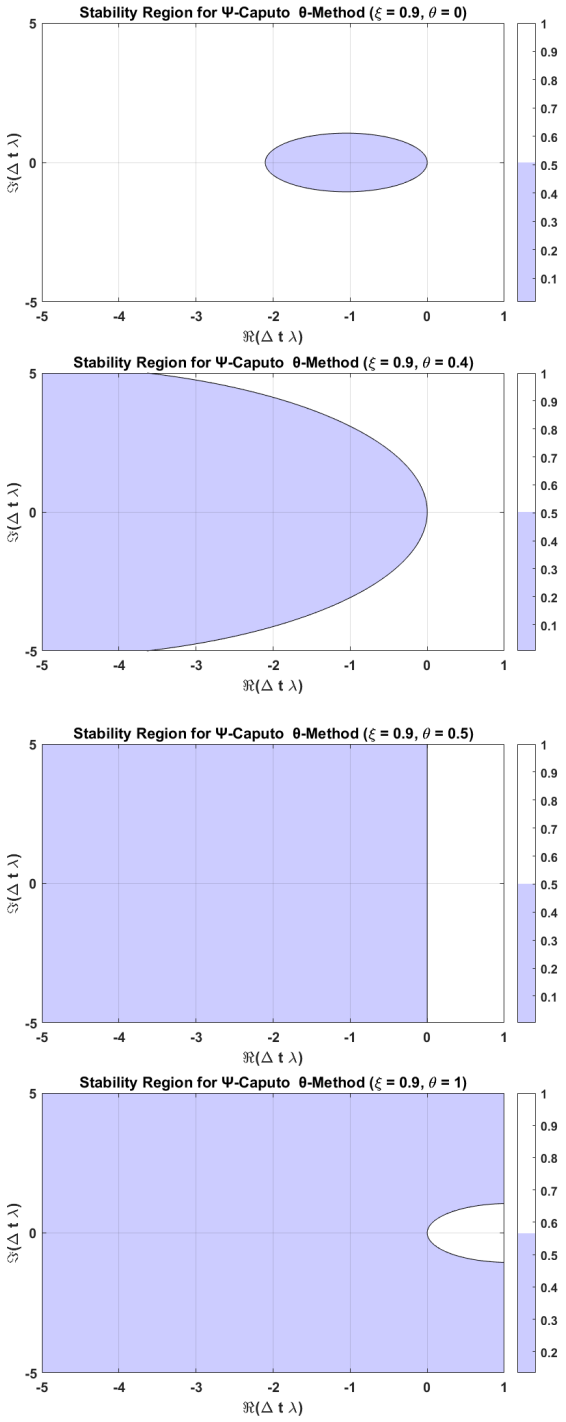

Figure 1. Stability Region for Ψ-Caputo θ-Method for different θ.

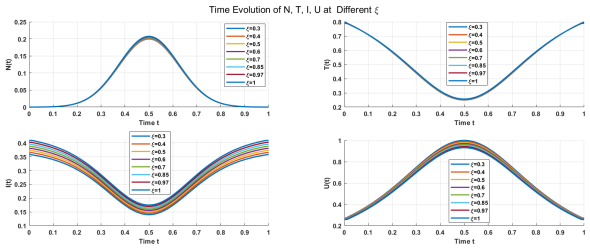

Figure 2. Numerical simulation at different values of fractional order ξ and $\Psi(t) = \exp(t^{0.5}), \theta = 0.5$.

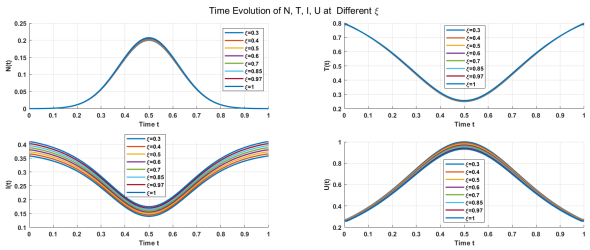

Figure 3. Numerical simulation at different values of fractional order ξ and $\Psi(t) = sin(t^{0.9}) + 1,\ \theta = 1$.

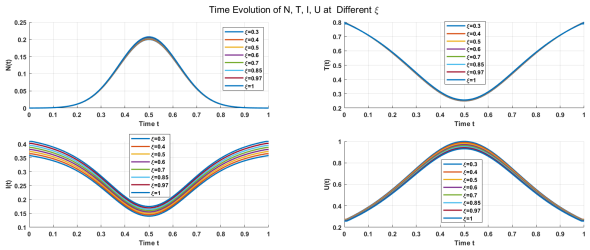

Figure 4. Numerical simulation at different values of fractional order ξ and $\Psi(t) = cos(0.9t) + t^0.7,\ \theta = 0.4$.

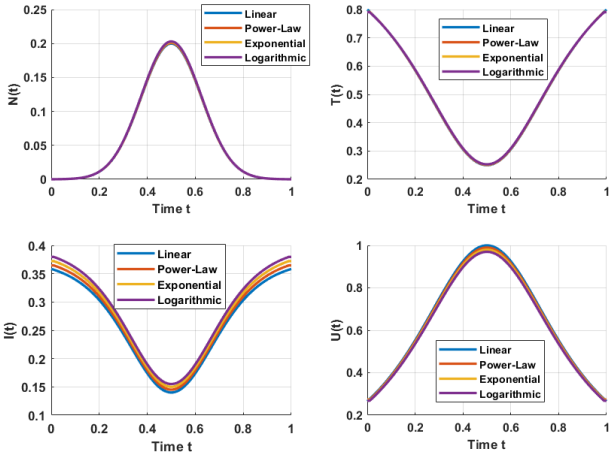

Figure 5. Numerical simulation at different values of kernel Ψ and$\alpha = 0.8, \theta = 0.5$, where,linear function $\Psi = t$, power-low function $\Psi = (0.90t + 0.50)^{0.5}$, exponential function $\Psi = exp(-t^{0.5}) + 1$, and logarithmic function $\Psi = log(1 + t) + 2$.

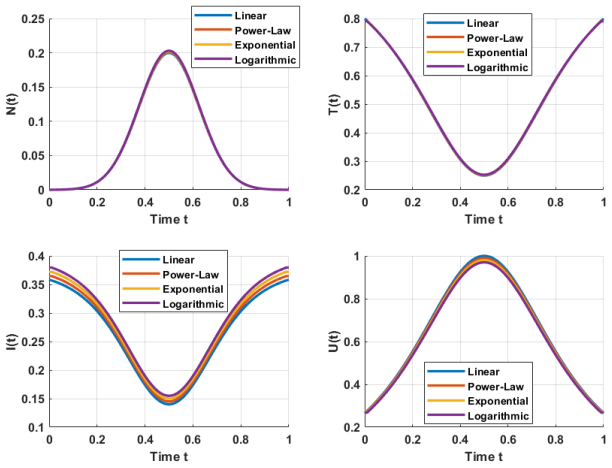

Figure 7. Numerical simulation at different values of kernel Ψ and$\alpha = 0.4, \theta = 1$, where,linear function $\Psi = t$, power-low function $\Psi = (0.90t + 0.50)^{0.5}$, exponential function $\Psi = exp(-t^{0.5}) + 1$, and logarithmic function $\Psi = log(1 + t) + 2$.

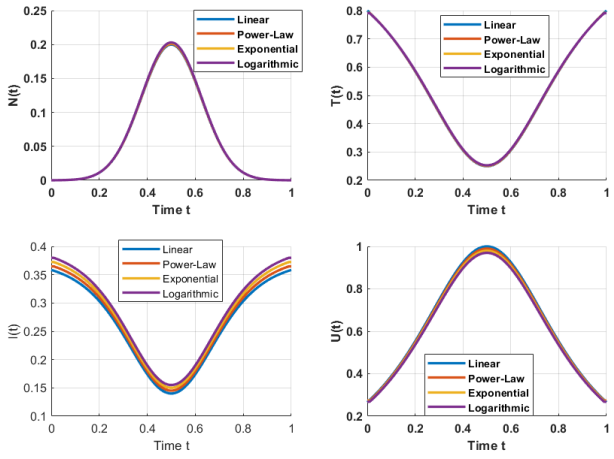

Figure 6. Numerical simulation at different values of kernel Ψ and$\alpha = 0.9, \theta = 0$, where,linear function $\Psi = t$, power-low function $\Psi = (0.90t + 0.50)^{0.5}$, exponential function $\Psi = exp(-t^{0.5}) + 1$, and logarithmic function $\Psi = log(1 + t) + 2$.

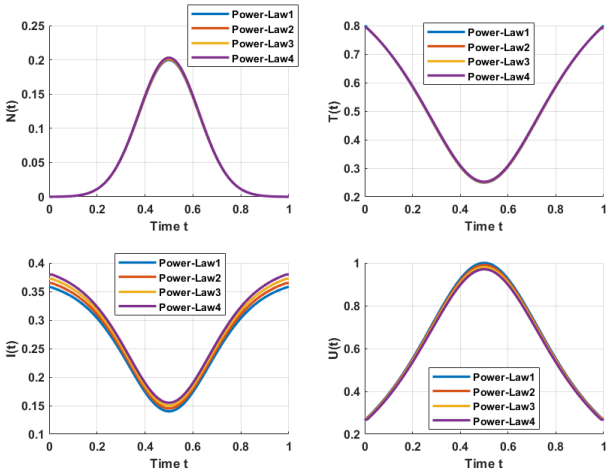

Figure 8. Numerical simulation at different values of power-low kernel Ψ and$\alpha = 0.7, \theta = 1$, where,power-low 1 function $\Psi = t^{0.5}$, power-low 2 function $\Psi = (0.80t + 1)^{0.4}$, power-low 3 function $\Psi = (0.80t - 1)^{0.4}$, and power-low 4 function $\Psi = (0.50t + 0.97)^{0.6}$.

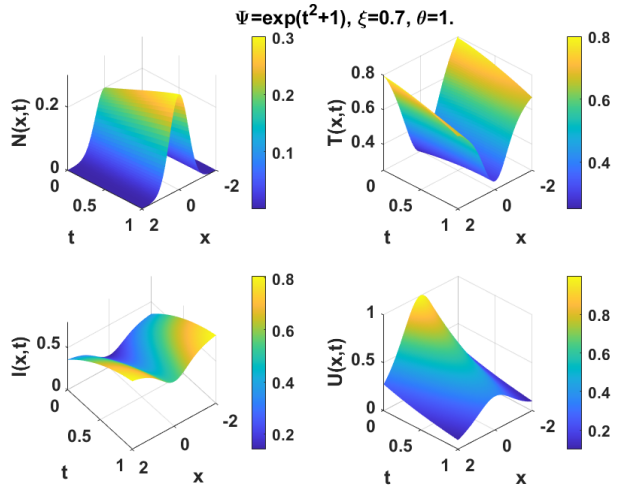

Figure 9. Numerical simulation in 3D using exponential function kernel.

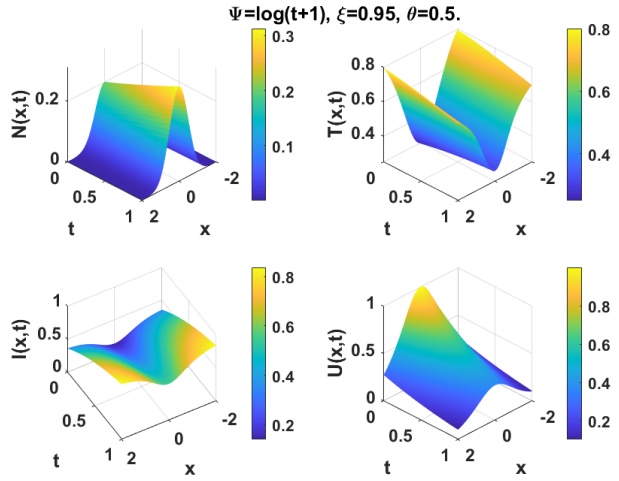

Figure 10. Numerical simulation in 3D using logarithmic function kernel.

REFERENCES

[1] D. Hanahan and R. A. Weinberg, "Hallmarks of cancer: The next generation," *Cell*, vol. 144, no. 5, pp. 646–674, 2011. DOI: 10.1016/j.cell.2011.02.013.

[2] R. L. Siegel, K. D. Miller, H. E. Fuchs, and A. Jemal, "Cancer statistics, 2022," *CA: A Cancer J. for Clin.*, vol. 72, no. 1, pp. 7–33, 2022. DOI: 10.3322/caac.21708.

[3] S. M. Al-Mekhlafi, "Numerical simulation of hybrid deterministic-stochastic pde models for cancer tumor growth," *Res. Math.*, vol. 12, no. 1, 2025. DOI: 10.1080/27684830.2025.2567717.

[4] J. A. Adam, "General aspects of modeling tumor growth and immune response," *Math. Comput. Model.*, vol. 23, no. 6, pp. 1–17, 1996. DOI: 10.1016/0895-7177(96)00028-6.

[5] N. Bellomo, N.-K. Li, and P. K. Maini, "On the foundations of cancer modelling: Selected topics, speculations, and perspectives," *Math. Model. Methods Appl. Sci.*, vol. 18, no. 4, pp. 593–646, 2008. DOI: 10.1142/S0218202508002796.

[6] I. Podlubny, *Fractional Differential Equations*. San Diego: Academic Press, 1999, ISBN: 9780125588409.

[7] A. A. Kilbas, H. M. Srivastava, and J. J. Trujillo, *Theory and Applications of Fractional Differential Equations*. Amsterdam: Elsevier, 2006, ISBN: 9780444518323.

[8] E. Ahmed and A. El-Sayed, "Fractional order model for cancer growth with immune response," *Math. Comput. Simul.*, vol. 162, pp. 1–10, 2019. DOI: 10.1016/j.matcom.2019.03.003.

[9] H. A. El-Saka, "Fractional-order epidemic models for tumor growth," *Chaos, Solitons & Fractals*, vol. 130, p. 109 399, 2020. DOI: 10.1016/j.chaos.2019.109399.

[10] K. Li and Y. Chen, "A fractional-order model for tumor angiogenesis under therapy," *Appl. Math. Comput.*, vol. 307, pp. 321–331, 2017. DOI: 10.1016/j.amc.2017.03.036.

[11] S. Kumar, R. Kumar, and J. Singh, "A time-fractional model for drug delivery in tumors with memory effects," *Chaos, Solitons & Fractals*, vol. 140, p. 110 246, 2020. DOI: 10.1016/j.chaos.2020.110246.

[12] R. Almeida, A. B. Malinowska, and M. T. T. Monteiro, "Fractional differential equations with a caputo derivative with respect to a kernel function and their applications," *Math. Methods Appl. Sci.*, vol. 41, no. 1, pp. 336–352, 2018. DOI: 10.1002/mma.4617.

[13] M. M. Abou Hasan, S. M. Al-Mekhlafi, H. A. Al-Ali, and F. Rihan, "Modeling hybrid crossover dynamics of immunochemotherapy and gene therapy: A numerical approach," *Math. Methods Appl. Sci.*, vol. 48, no. 4, pp. 8925–8938, 2025. DOI: 10.1002/mma.10765.

[14] S. M. Al-Mekhlafi, M. M. Abou Hasan, H. A. Al-Ali, and Z. Mukandavire, "A crossover optimal control framework for a time-delayed fractional-order diabetes model: Stability, bifurcation, and numerical analysis," *Math. Methods Appl. Sci.*, vol. 48, no. 17, pp. 15 723–15 741, 2025. DOI: 10.1002/mma.70046.

[15] M. M. Abou Hasan, A. M. Alghanmi, S. M. Al-Mekhlafi, H. Al-Ali, and Z. Mukandavire, "A novel crossover dynamics of variable-order fractal-fractional stochastic diabetes model: Numerical simulations," *J. Math.*, vol. 2025, pp. 1–22, 2025. DOI: 10.1155/jom/2986543.

[16] M. M. Abou Hasan, E. Ahmed, A. Ghaleb, M. S. Abou-Dina, and G. C. Georgiou, "Numerical solution of the newtonian plane couette flow with linear dynamic wall slip," *Fluids*, vol. 9, no. 8, p. 172, 2024. DOI: 10.3390/fluids9080172.

[17] F. Ansarizadeh, M. Singh, and D. Richards, "Modelling of tumor cells regression in response to chemotherapeutic treatment," *Appl. Math. Model.*, vol. 48, pp. 96–112, 2017. DOI: 10.1016/j.apm.2017.04.001.

[18] K. Diethelm, "An extension of the grönwall inequality to fractional differential equations," *Electron. J. Differ. Equations*, vol. 2008, no. 48, pp. 1–9, 2008.

[19] Y. Zhou, M. Song, and J. Peng, "Existence and uniqueness results for fractional differential equations with Ψ-hilfer derivative," *Adv. Differ. Equations*, vol. 2016, p. 283, 2016. DOI: 10.1186/s13662-016-0898-3.

[20] M. Aslefallah and M. Rostamy, "Numerical solution for poisson fractional equation via finite differences theta-method," *J. Math. Comput. Sci.*, vol. 10, pp. 241–252, 2014.

[21] E. Sousa and C. Li, "A weighted finite difference method for the fractional diffusion equation based on the riemann–liouville derivative," *Appl. Numer. Math.*, vol. 90, pp. 22–37, 2015. DOI: 10.1016/j.apnum.2014.11.006.